Molecular Pharmacology Fast Forward. Published on June 30, 2005 as doi:10.1124/mol.105.013888
This article has not been copyedited and formatted. The final version may differ from this version.

N-methyl-N'-nitro-N-nitrosoguanidine activates cell cycle arrest through distinct mechanisms activated in a dose-dependent manner

Dillon I. Beardsley, Wan –Ju Kim and Kevin D. Brown

Department of Biochemistry and Molecular Biology
and the UF Shands Cancer Center,
University of Florida College of Medicine,
Gainesville, FL 32610

Molecular Pharmacology Fast Forward. Published on June 30, 2005 as DOI: 10.1124/mol.105.013888
This article has not been copyedited and formatted. The final version may differ from this version.

MOLPHARM/2005/013888

Running Title Page

Running Title: ATR/Chk1 pathway controls high-dose MNNG response

Correspondence: Dr. K.D. Brown
Dept. of Biochemistry and Molecular Biology
University of Florida College of Medicine
1600 SW Archer Road, Box 100245
Gainesville, FL 32610

Phone (352) 273-5458
Fax (352) 392-1445
Email kdbrown1@ufl.edu

Text Contents
Text: 28 pages
Figures: 6
Tables: 0

Word Count
Abstract: 192
Introduction: 749
Discussion: 1,542

Abbreviations:

MNNG, N-methyl-N'-nitro-N-nitrosoguanidine

ATM, Ataxia-Telangiectasia, mutated

ATR, ATM and Rad-3 related

DSB, double strand break

AP, apurinic/apyrimidinic

MMR, mismatch repair

RNAi, RNA interference

siRNA, short-interfering RNA

BER, base excision repair

Molecular Pharmacology Fast Forward. Published on June 30, 2005 as DOI: 10.1124/mol.105.013888
This article has not been copyedited and formatted. The final version may differ from this version.

Abstract

S_N1 alkylating agents, such as the mutagenic and cytotoxic drug N-methyl-N'-nitro-N-nitrosoguanidine (MNNG), robustly activate the DNA damage-responsive G2 checkpoint. Establishment of this checkpoint is dependent on a functional mismatch repair (MMR) system; however, exposure to high doses of MNNG overrides the requirement for MMR to trigger G2 arrest. Also, unlike moderate-dose exposure where the G2 checkpoint is attenuated in ATM-deficient cells, high-dose MNNG treatment activates G2 arrest through an ATM-independent mechanism. We document that this arrest is sensitive to the pharmacological agents caffeine and UCN-01 that inhibit the checkpoint kinases ATM/ATR and Chk1/Chk2, respectively. Further, these agents block inactivation of the cell cycle regulatory molecules Cdc25C and Cdc2, establishing the downstream mechanism through which high-dose MNNG establishes G2 arrest. Activation of both Chk2 and Chk1 was independent of ATM and MMR in response to high-dose MNNG unlike response to moderate doses of this drug. Chk2 was found to be dispensable for cell cycle arrest in response to high-dose MNNG treatment; however, ATR-deficiency and decreased Chk1 expression forced by RNA interference resulted in diminished checkpoint response. These results indicate that MNNG activates the G2 checkpoint through different mechanisms activated in a dose-dependent fashion.

Molecular Pharmacology Fast Forward. Published on June 30, 2005 as DOI: 10.1124/mol.105.013888
This article has not been copyedited and formatted. The final version may differ from this version.

Introduction

N-methyl-N'-nitro-N-nitrosoguanidine (MNNG) is a nitrosourea and a monofunctional S_N1 alkylating agent. MNNG and related genotoxic agents are extremely mutagenic, carcinogenic, and evoke a strong cell cycle arrest and/or apoptotic response. MNNG methylates various nucleophilic centers within the DNA molecule with methylation of the N^3 position of adenine and the N^7 and O^6 position of guanine being the predominant lesions. N^3MeA and N^7MeG lesions are efficiently repaired by base excision repair (BER). However, the cytotoxic and mutagenic properties of MNNG are thought to principally stem from the methylation of the O^6 position of guanine (Karran and Bignami, 1992; Stojic et al., 2004a). Direct repair of mutagenic O^6MeG lesions is accomplished by the repair protein methylguanine-DNA methyltransferase (MGMT). Accordingly, lost or diminished MGMT activity results in MNNG-induced increased lesion load and sensitivity to MNNG (Kalamegham et al., 1988).

In addition to direct repair, O^6MeG lesions are recognized by the mismatch repair (MMR) system (Duckett et al., 1996; Griffin et al., 1994). MMR is an evolutionarily conserved DNA repair mechanism that is chiefly responsible for resolving post-replicative mismatches in DNA (Modrich and Lahue, 1996). Furthermore, MMR has been proposed to play an active role during response to MNNG-induced DNA damage. Specifically, exposure to MNNG and related methylators results in robust establishment of G2 arrest and MMR-deficient cells are unable to activate either cell cycle arrest and/or apoptosis in response to these drugs (Goldmacher et al., 1986; Kat et al., 1993; Koi et al., 1994; Meikrantz et al., 1998). The inability of MMR-deficient cells to respond to MNNG-induced genotoxic insult has been termed alkylation tolerance (Branch et al., 1993; Kat et al., 1993).

The molecular basis of the alkylation-tolerant phenotype and the mechanistic involvement of the MMR system in growth arrest or apoptogenic signaling is the subject of much attention. Several groups observed, in response to MNNG, that MMR-deficient cells display defective ATR-dependent activation of the kinase Chk1 (Adamson et al., 2005; Stojic et al., 2004b; Wang and Qin, 2003). Our lab has recently determined, in response to a moderate MNNG dose, that MMR-deficient cells display both faulty Chk1

and Chk2 activation and that both these kinases are required to fully activate G2 arrest (Adamson et al., 2005).

The structurally unrelated Chk1 and Chk2 kinases both phosphorylate the cell cycle regulatory Cdc25C phosphatase at the Ser216 residue *in vitro* (Ahn et al., 2000; Matsuoka et al., 2000; Sanchez et al., 1997). Phosphorylation of Cdc25C consequently targets this protein for interaction with 14-3-3 proteins that facilitate Cdc25C nuclear export (Lopez-Girona et al., 1999; Peng et al., 1997). Removal of Cdc25C from the nuclear compartment relieves inhibitory phosphorylation of the cyclin-dependent kinase Cdc2 (Lee et al., 1992; Strausfeld et al., 1991). Thus, Chk1/Chk2-induced Cdc25C inhibition forms a molecular basis for the G2 checkpoint by inhibiting activation of Cdc2 and restricting entry into mitosis.

Activation of Chk2 in response to γ-irradiation is dependent upon direct phosphorylation by the ATM kinase (Ahn et al., 2000; Matsuoka et al., 2000). Conversely, the ATM and Rad-3-related kinase ATR activates Chk1 in response to genotoxic insult (Liu et al., 2000; Zhao and Piwnica-Worms, 2001). Both ATR and Chk1 are required for activation of the G2 checkpoint in response to IR and other genotoxins (Liu et al., 2000; Sanchez et al., 1997; Zhao and Piwnica-Worms, 2001). In contrast, cells deficient in ATM show no gross defects in the triggering of G2 arrest in response to IR; rather, ATM-deficient cells are unable to arrest advance into mitosis immediately after γ-irradiation (Paules et al., 1995; Xu et al., 2002). Likewise, cells deficient in Chk2 are able to trigger the G2/M checkpoint in response to IR (Jallepalli et al., 2003). These findings support the view that the ATR/Chk1 pathway is the dominant mechanism controlling the G2 checkpoint in response to γ-irradiation. However, several recent reports have highlighted a role for Chk2 in triggering G2 arrest in response to various stimuli (Castedo et al., 2004; Masrouha et al., 2003; Singh et al., 2004; Wei et al., 2005).

During our previous investigation focused on the molecular basis of MMR-dependent cell cycle arrest in response to MNNG we documented that MMR-deficient cell lines treated with a high-dose of this drug robustly activated the G2 checkpoint. Other groups have also observed MMR-independent activation of this checkpoint in cells treated with high doses of MNNG (Jaiswal et al., 2004; Stojic et al., 2005). Here we report the

Molecular Pharmacology Fast Forward. Published on June 30, 2005 as DOI: 10.1124/mol.105.013888
This article has not been copyedited and formatted. The final version may differ from this version.

mechanisms responsible for this high-dose response and contrast these results with the pathways controlling response to moderate doses of this alkylating agent.

Materials and Methods

Cell culture and drug treatment

The SV40-immortalized A-T fibroblast line AT22IJE-T stably expressing full-length recombinant human ATM (designated YZ-5) or stably transfected with empty vector (designated EBS-7) were cultured as previously indicated (Ziv et al., 1997). The MLH1-deficient human colorectal adenocarcinoma line HCT116 and its derivative (HCT116+ch3) were cultured with or without 400 μg/ml G418 as previously outlined (Koi et al., 1994; Umar et al., 1997). $ATR^{flox/-}$ cells (Cortez et al., 2001) were obtained from Dr. S. Elledge (Baylor College of Medicine). To abrogate ATR expression in these cells, 1.0 μL ($1X10^6$ PFU/ μL) of adenovirus expressing Cre recombinase (Ad-Cre) was added to to cultures for two days. HCT116 $Chk2^{-/-}$ (Jallepalli et al., 2003) were obtained from Drs. B. Vogelstein and F. Bunz (Johns Hopkins Cancer Center). All cell lines were grown at 37°C in a humidified 5% CO_2 incubator. ATM, ATR, Chk2, or MLH1 expression was confirmed in appropriate mutant and control lines by immunoblotting.

MNNG treatment was performed by removing media from cultures of logarithmically growing cells and adding serum-free media. MNNG was then added to the indicated final concentration and cells returned to the incubator. After a 1 hr drug exposure, the plates were rinsed extensively with PBS, cells were re-fed on complete growth media and returned to the incubator. MNNG (Aldrich) was dissolved in 0.1 M Na-acetate (pH 5.0) at a stock concentration of 10 mM and stored at –20 ^oC. UCN-01 (7-hydroxystaurosporine) was obtained from the Developmental Therapeutics Program of the National Cancer Institute, NIH. A 10 mM stock solution of this drug was stored at –80 ^oC. UCN-01 was added to cell cultures (500 nM final concentration) 45 min before MNNG treatment. Cells were maintained on UCN-01 both during and after MNNG exposure until cells were harvested and analyzed. Caffeine (Sigma) was diluted in PBS at a stock concentration of 100 mM and stored at RT. Caffeine (5 mM final concentration) was added 1 hr prior to MNNG treatment, and was maintained in the

Molecular Pharmacology Fast Forward. Published on June 30, 2005 as DOI: 10.1124/mol.105.013888
This article has not been copyedited and formatted. The final version may differ from this version.

medium during and after MNNG exposure.

Flow cytometry

For quantitative analysis of cellular DNA content by flow cytometry, cells were harvested by trypsinization, washed with PBS, fixed in ice-cold 70% ethanol and stored at –20^{o}C for a minimum of 24 hr. Prior to analysis, cells were washed twice in PBS followed by a 30 min room temperature (RT) incubation in PBS containing 25 μg/ml propidium iodide (PI) and 100 μg/ml RNase A. Cells were analyzed using a Becton Dickenson FACSCalibur flow cytometer and >10,000 events plotted using CellQuest software. Cell cycle distribution was calculated using ModFit LT 3.0 software.

Immunoblot Analysis

SDS-PAGE and immunoblotting procedures were conducted as previously outlined (Adamson et al., 2002). Membranes were probed with antibodies directed against total ATM (AM-9, (Allen et al., 2001), total Chk1 (sc-8408, Santa Cruz Biotechnology), phospho-Ser317 Chk1 (2344, Cell Signaling), total Chk2 (sc-17748, Santa Cruz Biotechnology), phospho-Thr68 Chk2 (sc-16297-R, Santa Cruz Biotechnology), total Cdc2 (sc-54, Santa Cruz Biotechnology), phospho-Tyr15 Cdc2 (9111, Cell Signaling), Cdc25C (sc-327, Santa Cruz Biotechnology), SMC1 (A300-055A, Bethyl Laboratories) or tubulin (DM1A, a gift of Dr. D.W. Cleveland, UCSD) as indicated. Peroxidase-conjugated secondary antibodies were obtained from Kirkegaard and Perry Labs (Gaintersburg, MD) and immunoblot signals detected using Pico-West chemiluminescent substrate (Pierce). Immunoblot signals were quantified using NIH Image (ver 1.63).

Anti-ATR antiserum was created in our laboratory by isolating a ~1.1 kb segment of the human ATR mRNA transcript by RT-PCR (nucleotide # 5294-6321 of the ATR ORF). Subsequently, this cDNA was subcloned as a BamHI/EcoRI fragment into the prokaryotic expression vector pGEX-4T and clones verified by automated sequencing. The encoded GST-ATR fusion protein (ATR aa# 1765-2107) was induced by addition of 1 mM IPTG to a logarithmically growing culture of TOP-10 (Invitrogen) *E. coli* harboring this plasmid. The fusion protein was found to be insoluble; thus, inclusion

Molecular Pharmacology Fast Forward. Published on June 30, 2005 as DOI: 10.1124/mol.105.013888
This article has not been copyedited and formatted. The final version may differ from this version.

bodies were isolated. This material was used to immunize 3 adult New Zealand White rabbits and one of these rabbits was found to display positive immunoreactivity by immunoblotting after initial immunization and 2 boosts at 3 week intervals. The resultant antiserum (pAb-ATR39) was used routinely at a dilution of 1:5,000 for immunoblot analysis. Rabbit immunization and housing was conducted by OpenBiosystems (Huntsville, AL).

Cell fractionation

Cells were separated into nuclear and cytoplasmic fractions using NE-PER Nuclear and Cytoplasmic Extraction Reagents as outlined by the manufacturer (Pierce). After lysing cells with supplied buffers, nuclei were harvested by centrifugation in a microcentrifuge (5 min; 16,000 x *g*; 4 ^{o}C). Cytoplasmic (supernatant) and nuclear (pellet) fractions were separated and stored at -80 ^{o}C prior to immunoblot analysis.

RNA interference

Pooled synthetic siRNA duplexes (SMARTpool siRNA) specific for Chk1 (cat# M-003255-02) and Non-targeting siRNA (cat# D-001210-01-20) were purchased from Dharmacon (Lafayette, CO). For siRNA transfection, HCT116 Chk2-/- or HCT116+ch3 cells were seeded into six-well tissue culture plates at a density of 5x10^{5} cells/well 24 hr prior to transfection. Just prior to transfection, medium was removed and 1 ml of complete growth medium (without antibiotics) was added to each well. Subsequently, 200 µl of reaction mix containing 5 µl of a 20 µM siRNA stock and 2 µl Oligofectamine (Invitrogen) diluted in Opti-MEM was added to each well. Following an O/N incubation at 37^{o}C, the cells were split at a 1:4 ratio, and then cultured O/N. The following day, the cells were transfected a second time as outlined above. Twenty four hr after the second transfection cells were washed, re-fed on complete growth medium and treated with 5 or 25 µM MNNG for 1 hr. MNNG-treated cells were cultured for 48 hr and subsequently harvested and fixed for flow cytometry or lysates formed for immunoblot analysis.

Molecular Pharmacology Fast Forward. Published on June 30, 2005 as DOI: 10.1124/mol.105.013888
This article has not been copyedited and formatted. The final version may differ from this version.

Results

High-dose MNNG exposure overrides ATM and MMR-dependent G2 arrest observed in response to moderate drug dose.

A previous study from our laboratory that addressed the mechanisms responsible for activating the G2 checkpoint in response to the S_N1 alkylating agent MNNG showed that this response was both ATM and MMR-dependent (Adamson et al., 2005). Specifically, treatment of matched ATM proficient/deficient and MMR proficient/deficient cell lines with a moderate-dose of MNNG (*i.e.,* 5 μM) resulted in a blunted checkpoint response in ATM-deficient cells and a complete abrogation of arrest in MMR-deficient cells. However, we also observed that cells deficient in ATM and MMR display normal arrest in response to an increased dose of MNNG. To illustrate this point, we treated the isogenic ATM-proficient, YZ-5 and ATM-deficient EBS-7 lines with 5μM MNNG and with 25μM MNNG (high-dose) and analyzed cells 48 hr after drug treatment by flow cytometry. G2 arrest was attenuated in the ATM-deficient EBS-7 cell line in response to 5μM MNNG (Fig. 1A) compared to response in the isogenic ATM-proficient YZ-5 line (Fig. 1B). In contrast, robust G2 arrest at this timepoint was observed following exposure to 25μM MNNG in both YZ-5 and EBS-7 cells.

MNNG response was also examined using the MMR-deficient HCT116 and MMR-proficient HCT116+ch3 colorectal tumor cell lines in parallel experiments. MMR-deficient HCT116 cells were unable to activate the G2 checkpoint 48 hr after exposure to 5μM MNNG treatment (Fig. 1C). In contrast, HCT116+ch3 cells displayed a robust G2 arrest in response to 5 μM MNNG exposure (Fig. 1D). Both HCT116 and HCT116+ch3 cells treated with 25μM MNNG displayed a substantial G2 arrest 48 hr after drug treatment (Fig. 1C,D, respectively). Taken together, these results indicate that high-dose MNNG treatment activates the G2 checkpoint through an ATM and MMR-independent mechanism(s). For clarity, we refer to moderate-dose MNNG exposure as the MNNG dose that activates a MMR-dependent G2 arrest, while high-dose exposure is that dose that activates a MMR-independent checkpoint response.

We previously determined that checkpoint response to moderate doses of MNNG was ablated by the pharmacological agents caffeine and UCN-01. Caffeine is a potent

Molecular Pharmacology Fast Forward. Published on June 30, 2005 as DOI: 10.1124/mol.105.013888
This article has not been copyedited and formatted. The final version may differ from this version.

inhibitor of the PIK-like protein kinase family (Sarkaria et al., 1999; Sarkaria et al., 1998), and two of the members of this family (ATM and ATR) are linked to genotoxin-induced activation of G2 arrest (Abraham, 2001). We pretreated EBS-7 and HCT116 cells with 5mM caffeine prior to 25 μM MNNG exposure and maintained the cells on 5 mM caffeine until the cells were harvested 48 hr after MNNG treatment and subsequently analyzed by flow cytometry. We observed that caffeine treatment resulted in near complete abrogation of G2 arrest in both EBS-7 (Fig. 1E) and HCT116 (Fig. 1F) when compared to cells treated with 25μM MNNG in the absence of caffeine. Cells treated with caffeine alone showed no G2 arrest consistent with this agent inhibiting damage-induced signaling.

UCN-01 (7-hydroxystaurosporine) is a strong inhibitor of the cell cycle kinase Chk1 (Graves et al., 2000) and the functionally related, yet structurally dissimilar, Chk2 kinase (Yu et al., 2002). Similar to caffeine treatment, EBS-7 and HCT116 cells were treated and maintained on 500nM UCN-01 after exposure to 25μM MNNG. We observed that UCN-01 abrogated G2 arrest 48 hr after 25μM MNNG exposure in both EBS-7 and HCT116 lines (Fig. 1E,F, respectively). Cells treated with UCN-01 only showed no apparent cell cycle arrest indicating that this drug is inhibiting signaling in response to MNNG. The results of these experiments using pharmacological inhibitors connect high-dose MNNG response and conserved ATM/ATR and Chk1/Chk2-dependent pathways.

High-dose MNNG exposure activates G2 arrest via inhibition of the cell cycle regulatory molecules Cdc25C and Cdc2.

Previous work from our laboratory indicated that G2 arrest in response to moderate doses of MNNG is attributable, at least in part, to inactivation of Cdc25C and Cdc2 (Adamson et al., 2005). Therefore, we next examined these downstream biochemical mechanisms during high-dose MNNG-induced response. Specifically, we assessed nuclear retention of the cell cycle phosphatase Cdc25C and accumulation of catalytically inactive cyclin-dependent kinase Cdc2 following 25 μM MNNG exposure. Analysis of isolated EBS-7 nuclei harvested 48 hr after 25μM MNNG demonstrated a striking decrease in the nuclear levels of Cdc25C in these cells following high-dose MNNG exposure (Fig. 2A). As shown previously (Adamson et al., 2005), this ATM-deficient

line does not dramatically downregulate nuclear levels of Cdc25C in response to 5 μM MNNG. While slight fluctuations in nuclear Cdc25C abundance were observed, these experiments clearly indicate that this molecule was maintained at a high level in cells treated with a combination of MNNG and caffeine or MNNG and UCN-01. These results indicate that these pharmacological inhibitors inhibit G2 arrest through a blockade of Cdc25C export from the nucleus in response to high-dose MNNG. Parallel experiments were carried out on the MMR-deficient HCT116 and identical results were obtained (Fig. 2B). These findings indicate that exposure to high-dose MNNG leads to marked decreases in Cdc25C abundance within the nucleus of both ATM and MMR-deficient cell lines at the time of optimal G2 arrest similar to ATM and MMR-proficient cell lines treated with moderate doses of MNNG (Adamson et al., 2005).

Next, whole cell lysates from MNNG treated EBS-7 and HCT116 cells were immunoblotted with the phospho-Tyr15 Cdc2 specific antibody. Phosphorylation of Cdc2 at residue Tyr15 inhibits the catalytic activity of this cyclin-dependent kinase and accumulation of Tyr15 phosphorylated Cdc2 is correlated with G2 arrest (Kharbanda et al., 1994). In EBS-7 cells treated with 5 μM MNNG we observed a modest accumulation of inactive Cdc2 (Fig 2C). This result is consistent with the attenuated checkpoint response displayed by this line in response to a moderate-dose of MNNG. In response to 25 μM MNNG, however, we observed a striking level of Tyr15-phosphorylated Cdc2 48 hr after drug. Accumulation of phosphorylated Cdc2 was blocked in cells pretreated and maintained on either caffeine or UCN-01 along with 25 μM MNNG exposure. These results indicate that these pharmacological inhibitors block G2 arrest through a block of Cdc2 inactivation. Again, similar results were obtained in parallel experiments conducted on HCT116 cells (Fig. 2D). The only notable difference between MNNG response in HCT116 and EBS-7 cells is that HCT116 cells show no increase in Tyr15-phosphorylated Cdc2 in response to 5 μM MNNG exposure. This finding is consistent with the abrogated checkpoint activation shown by this MMR-deficient line following 5 μM MNNG treatment. In sum, these findings indicate that, similar to response to a moderate MNNG dose, high-dose MNNG exposure activates G2 arrest through inactivation of both Cdc25C and Cdc2.

Molecular Pharmacology Fast Forward. Published on June 30, 2005 as DOI: 10.1124/mol.105.013888
This article has not been copyedited and formatted. The final version may differ from this version.

Activation of Chk1 and Chk2 do not require either ATM or MMR in response to high-dose MNNG treatment.

We recently reported that in response to a moderate-dose of MNNG that activation/phosphorylation of both Chk1 and Chk2 occurs in a MMR-dependent manner while Chk2 activation also requires ATM activity (Adamson et al., 2005). To determine if Chk1 and/or Chk2 are activated during response to high-dose MNNG exposure, we assessed the phosphorylation state of these molecules in EBS-7 and HCT116 cells following treatment with 25 μM MNNG. Immunoblot analysis of extracts formed from 25 μM MNNG treated EBS-7 cells with phospho-Ser317 Chk1-specific antibody, a post-translational modification linked to catalytic activation of this kinase (Zhao and Piwnica-Worms, 2001), detected an increase in Chk1 phosphorylation with 5μM MNNG treatment (Fig. 3A). This agrees with previous findings indicating that Chk1 activation occurs in an ATM-independent manner in response to MNNG. However, we measured a notable increase in Chk1 phosphorylation (1.9-fold) in extracts from EBS-7 cells treated with 25 μM compared to those exposed to 5μM MNNG. In MMR-deficient HCT116 cells, we again observed no Chk1 activation in response to 5μM MNNG (Fig. 3B). However, robust Chk1 Ser317 phosphorylation was evident in these cells in response to 25 μM MNNG. These experiments indicate that, when compared to the response mounted following exposure to a lower dose of MNNG, high-dose MNNG exposure results in heightened Chk1 activity in EBS-7 cells, and promotes activation of Chk1 through a MMR-independent mechanism.

Extracts from MNNG treated EBS-7 and HCT116 cells were also assayed for phosphorylation of the Thr68 residue of Chk2. Phosphorylation of this residue is linked to activation of the Chk2 kinase (Matsuoka et al., 2000). EBS-7 cells displayed no Chk2 phosphorylation in response to 5μM MNNG, reinforcing the ATM-dependency of Chk2 phosphorylation in response to moderate doses of MNNG (Fig. 3C). However, prominent phosphorylation of Chk2 was detected in EBS-7 cells treated with 25μM MNNG. As previously shown, HCT116 cells treated with 5 μM MNNG exhibited no detectable Chk2 phosphorylation (Fig. 3D). However, exposure to 25μM MNNG

Molecular Pharmacology Fast Forward. Published on June 30, 2005 as DOI: 10.1124/mol.105.013888
This article has not been copyedited and formatted. The final version may differ from this version.

resulted in significant Chk2 phosphorylation. These results indicate that, unlike the MMR and ATM-dependent nature of Chk2 phosphorylation/activation observed in response to moderate doses of MNNG, activation of Chk2 in response to high-dose MNNG exposure is not dependent upon either ATM or MMR.

ATR is required for Chk1 activation and establishment of G2 arrest in response to high-dose MNNG exposure

In light of the inhibitory effect of caffeine on G2 arrest and the ATM-independent nature of both checkpoint activation and Chk1 and Chk2 activation, we hypothesized that ATR activity is essential to triggering G2 arrest in response to high-dose MNNG exposure. To address this question, we tested the $ATR^{flox/-}$ cell line (Cortez et al., 2001). This cell line is a derivative of HCT116 that contains one disrupted ATR allele and the other ATR allele has been engineered to contain loxP sites flanking exon 2. Expression of Cre recombinase results in efficient excision of exon 2 resulting introduction of a frameshift mutation within the ATR transcript and consequential premature truncation of the ATR protein. Therefore, Cre recombinase expression results in conditional loss of ATR expression. Treatment of the parental HCT116 line with adenovirus encoding Cre recombinase (Ad-Cre) for 48 hr resulted in no detectable decrease in ATR expression (Fig. 4A, *top*). As previously shown (Cortez et al., 2001), ATR abundance in uninfected $ATR^{flox/-}$ cells was diminished compared to the parental HCT116 line containing two functional ATR alleles and Ad-Cre infection of $ATR^{flox/-}$ cells resulted in a dramatic decrease in ATR abundance. To assure ATM expression was unaltered in these cells, these extracts were also immunoblotted with anti-ATM (Fig. 4A, *middle*). Both HCT116 and $ATR^{flox/-}$ lines displayed no detectable alterations in ATM expression regardless of Ad-Cre infection.

Next, we immunoblotted extracts of MNNG-treated $ATR^{flox/-}$ cells with phospho-specific Chk1 and Chk2 antibodies. We observed activation of Chk1 following 25 μM MNNG treatment in $ATR^{flox/-}$ cells not infected with Ad-Cre (Fig. 4B). After Ad-Cre infection, however, $ATR^{flox/-}$ cells displayed no detectible Chk1 activation in response to 25μM MNNG. Further, Ad-Cre infection alone had no detectable effect on the accumulation of phosphorylated Chk1. These lysates were also assessed for Chk2

Molecular Pharmacology Fast Forward. Published on June 30, 2005 as DOI: 10.1124/mol.105.013888
This article has not been copyedited and formatted. The final version may differ from this version.

phosphorylation/activation. Again, we observed significant Chk2 phosphorylation in response to 25 μM MNNG in uninfected $ATR^{flox/-}$ cells (Fig. 4C). Further, no Chk2 phosphorylation was observed in response to Ad-Cre infection alone. In direct contrast to Chk1 phosphorylation, robust phosphorylation of Chk2 was observed following 25μM MNNG in Ad-Cre infected in $ATR^{flox/-}$ cells. These results argue against a strict requirement for ATR in activation of Chk2 in response to 25μM MNNG and since ATM is present in these cells (see Fig. 4A) it is likely that Chk2 is activated by ATM in ATR-deficient cells.

Flow cytometry was subsequently performed in uninfected and Ad-Cre infected $ATR^{flox/-}$ cells and HCT116 cells treated in parallel. We observed typical robust G2 arrest (73%) 48 hr after 25μM MNNG treatment in the parental HCT116 cell line (Fig. 4D). Further, MNNG-induced G2 arrest in HCT116 was unaltered by infection with Ad-Cre. In uninfected $ATR^{flox/-}$ cells, exposure to 25 μM MNNG resulted in less robust accumulation of cells arrested in G2 (51%) compared to the response observed uninfected HCT116. This outcome is likely the result of decreased expression of ATR in the $ATR^{flox/-}$ cells compared to the parental line. Consistent with this interpretation, a reduction in G2 arrest (28%) was observed in MNNG-treated, Ad-Cre infected $ATR^{flox/-}$ cells. In both HCT116 and $ATR^{flox/-}$ lines we found that Ad-Cre infection alone did not induce G2 arrest. Analysis of three independent experiments (Fig. 4F) indicate that 25 μM MNNG-treated $ATR^{flox/-}$ cells display a statistically significant decrease in G2 arrest (p=0.005, Student's t-Test, 2 sided) compared to MNNG treated HCT116 cells and Ad-Cre infection of $ATR^{flox/-}$ cells resulted in a highly significant decrease in MNNG-induced G2 arrest ($p=2.5\times10^{-5}$) compared to HCT116. The interpretation that this diminished G2 arrest is attributable to reduced ATR expression is supported by the observation that MNNG-treated, Ad-Cre infected $ATR^{flox/-}$ cells display a significant (p=0.002) reduction in G2 arrest when compared to uninfected MNNG-treated $ATR^{flox/-}$ cells. Since measurable G2 arrest was observed in MNNG-treated, Ad-Cre infected $ATR^{flox/-}$ cells we cannot strictly conclude that ATR is sufficient to induce G2 arrest in response to high-dose MNNG exposure. However, from these findings, we do conclude that ATR is required for activation of Chk1, but not Chk2, and that ATR, but not ATM, is required for establishing G2 arrest in response to high-dose MNNG exposure.

Molecular Pharmacology Fast Forward. Published on June 30, 2005 as DOI: 10.1124/mol.105.013888
This article has not been copyedited and formatted. The final version may differ from this version.

High-dose MNNG-induced G2 arrest is Chk2-independent

Findings outlined above indicate that the cell cycle arrest triggered by high-dose MNNG exposure is ATR-dependent and that this correlates with ATR-dependent Chk1 activation. However, Chk2 was robustly phosphorylated/activated in response to 25μM MNNG. To test a potential role for Chk2 in activation of G2 arrest in response to high-dose MNNG exposure we obtained an HCT116 derivative cell line deficient in Chk2 (Jallepalli et al., 2003). Immunoblot analysis of these cells confirmed Chk2-deficiency and indicated that Chk1 abundance was unaltered in HCT116 Chk2$^{-/-}$ cells (Fig. 5A). In response to 25μM MNNG exposure, HCT116 Chk2$^{-/-}$ cells exhibited a robust (66%) G2 arrest 48 hr after drug. Additionally, pretreatment and maintenance of these cells on UCN-01 during and after 25μM MNNG treatment completely abrogated G2 arrest in this cell line (Fig. 5B). As a result of this finding we conclude that the ATM/Chk2 pathway is not required for G2 checkpoint signaling in response to high doses of MNNG.

Chk1 is required for establishment of G2 arrest following high-dose MNNG exposure

Results outlined above indicate the importance of ATR in activation of the G2 checkpoint in response to high-dose MNNG exposure. To ascertain that the ATR/Chk1 pathway is involved in triggering high-dose MNNG-induced G2 arrest, we used RNA interference (RNAi) technology to reduce Chk1 expression in cultured cells. Initially, we used HCT116 Chk2$^{-/-}$ cells to uniquely isolate the role of Chk1 in activating this checkpoint. Immunblot analysis of HCT116 Chk2$^{-/-}$ cells transfected with pooled, Chk1-specific siRNA duplexes documented a 2.5-fold reduction of total Chk1 as compared to mock-transfected (no siRNA) or control-transfected (non-target siRNA) cells (Fig. 6A). When these cells were treated with 25 μM MNNG and assayed by flow cytometry 48 hrs post-drug, we observed that mock- and control-transfected cells displayed a robust G2 blockade (63%) (Fig. 6B). Cells transfected with Chk1-specific siRNA and subsequently treated with 25μM MNNG displayed a reduced percentage of cells in G2 (52%). This ~16% reduction in G2 arrested cells supports the notion that Chk1 is a necessary molecular component in the G2 checkpoint pathway activated in response to high-dose MNNG.

Molecular Pharmacology Fast Forward. Published on June 30, 2005 as DOI: 10.1124/mol.105.013888
This article has not been copyedited and formatted. The final version may differ from this version.

While consistently reproducible, the reduction in G2 arrest produced by siRNA-mediated Chk1 depletion was notably modest compared to results obtained on Chk1 siRNA-transfected cells treated with 5 μM MNNG (Adamson et al., 2005). In this previous study, we observed a reproducible ~50% reduction in 5 μM MNNG-induced G2 arrest in HCT116+ch3 cells transfected with Chk1 siRNA. We hypothesized that the more subtle effects observed in 25 μM treated cells are attributable to increased Chk1 catalytic activity in 25 μM treated cells when compared to Chk1 activity in 5 μM MNNG treated cells. This thinking stemmed from our observation that the accumulation of phosphorylated/activated Chk1 in MNNG-treated EBS-7 cells is 1.9-fold higher in 25 μM treated cells than in 5 μM-treated cells (see Fig. 3A). To confirm that this dose-dependent increase in Chk1 phosphorylation/activation is a general phenomenon, we treated HCT116+ch3 cells with 5 and 25 μM MNNG and subjected lysates from these cells to immunoblot analysis with phospho-Ser317 Chk1 specific antibody. Similar to our previous findings using EBS-7 cells, we observed that HCT116+ch3 cells treated with 25 μM MNNG displayed a 2.2-fold elevated level of phosphorylated/activated Chk1 when compared to cells treated with 5 μM MNNG (Fig. 6C). From these observations we conclude that higher doses of MNNG trigger a more robust activation of Chk1.

Next, we conducted flow cytometry analysis on Chk1 siRNA-transfected HCT116+ch3 cells treated with either 5 or 25 μM MNNG. We observed, in close agreement with results obtained from similarly manipulated HCT116 Chk2$^{-/-}$ cells, that transfection with pooled, Chk1-specific siRNA resulted in a 4.9-fold reduction in Chk1 expression in HCT116+ch3 cells compared to compared to mock- and control siRNA-transfected cells (Fig. 6D). Further, flow cytometry analysis of mock- and control siRNA-transfected HCT116+ch3 cells treated with either 5 or 25 μM MNNG indicated that these manipulations resulted in no apparent diminishment in G2 arrest at either MNNG dose (Fig. 6E). Flow cytometry also revealed that Chk1 depleted HCT116+ch3 cells treated with 5 μM MNNG showed a 37% reduction in G2 arrested cells compared to mock-transfected cells treated with this dose of MNNG. In contrast, and consistent with results from experiments on HCT116 Chk2$^{-/-}$ cells, Chk1 siRNA-transfected HCT116+ch3 cells treated with 25 μM MNNG displayed a 20% reduction in G2 arrested

Molecular Pharmacology Fast Forward. Published on June 30, 2005 as DOI: 10.1124/mol.105.013888
This article has not been copyedited and formatted. The final version may differ from this version.

cells compared to 25 μM MNNG treated, mock-transfected cells. Analysis of three independent experiments indicate that siRNA-mediated knockdown of Chk1 expression in 25 μM MNNG-treated HCT116+ch3 cells led to a statistically-significant decrease in G2 arrest (p=0.012) when compared to 25 μM MNNG-treated HCT116+ch3 cells transfected with control siRNA. Further, 25 μM MNNG-treated HCT116+ch3 cells transfected with Chk1 siRNA showed a highly significant (p=7.8x10^{-5}) reduction in G2 arrest when compared with 25 μM MNNG-tretaed HCT116+ch3 cells transfected with control siRNA. Of note, a statistically significant (p=0.005) difference between the percentage of G2 arrested cells in populations of Chk1 siRNA-transfected HCT116+ch3 cells treated with 5 or 25 μM MNNG was observed. From these experiments we conclude that siRNA-mediated knock-down of Chk1 produces a more significant effect on G2 arrest in response to moderate doses of MNNG compared to response to high-dose MNNG exposure. Moreover, it is reasonable to speculate that this effect stems, in part, from heightened Chk1 activity in cells treated with higher doses of this alkylating agent.

DISCUSSION

MNNG-induced checkpoint signaling: High vs. moderate-dose response

It has long been established that G2 checkpoint activation in response to S_N1 alkylating agents is triggered via a MMR-dependent mechanism (Goldmacher et al., 1986; Hawn et al., 1995; Kat et al., 1993; Koi et al., 1994). We, and others (Jaiswal et al., 2004; Stojic et al., 2005), have observed, however, that substantially higher doses of MNNG triggered G2 arrest in MMR-deficient cells. Here we document that, in cells treated with high-dose MNNG, both Chk1 and Chk2 are activated in a MMR-independent fashion, the MNNG-induced G2 checkpoint occurs independently of ATM, Chk2 and MMR, and checkpoint establishment is reliant upon the ATR/Chk1 signaling pathway. When compared with earlier studies that examined mechanisms responsible for MMR-dependent G2 arrest (Adamson et al, 2005; Stojic et al, 2004b), we conclude that MNNG activates the G2 checkpoint through various pathways and these different mechanisms are activated in a dose-dependent manner.

We observed that caffeine and UCN-01 blocked establishment of the G2 checkpoint in response to high-dose MNNG exposure. These drugs exerted similar effects in

response to moderate doses of MNNG (Adamson et al., 2005). Here, we also examined the effects of these agents on two downstream events linked to G2 checkpoint establishment; namely, Cdc25C and Cdc2 inactivation. Our previous work demonstrated that inactivation of these molecules in response to moderate doses of MNNG was dependent upon a functional MMR system indicating that Cdc25C and Cdc2 are targeted for inactivation in response to MNNG (Adamson et al., 2005). Our present findings indicate that Cdc25C and Cdc2 are also inactivated in response to high-dose MNNG exposure; thus, both moderate-dose and high-dose response utilize, at least in part, similar downstream mechanisms to block cell cycle advance. However, it bears consideration that other G2 checkpoint pathways may be activated in response to MNNG and other genotoxic drugs. Clearly, additional investigation is required to fully elucidate the mechanisms that halt cell cycle advance at the G2/M transition point.

One of the prominent dissimilarities between response to moderate doses of MNNG (MMR-dependent G2 arrest activated) and high doses of MNNG (MMR-independent G2 arrest activated) is differences in Chk1 and Chk2 activation. In response to IR, Chk2 is activated by ATM through phosphorylation of the Thr68 residue (Matsuoka et al., 2000). Matsuoka *et al* (Matsuoka et al., 1998) also determined that Chk2 was activated in an ATM-independent manner in response to hydroxyurea and UV light and that this was most likely attributable to ATR activity. Here, we document that Chk2 activation is ATM-independent during high-dose MNNG response and since ATR is activated in response to MNNG, it is plausible that ATR is responsible for the Chk2 phosphorylation observed in ATM-deficient cells following high-dose MNNG exposure. ATM-independent Chk2 activation also occurs in response to high-dose IR exposure (Matsuoka et al., 1998), suggesting that dose-responsive activation of Chk2 by ATR may be a general phenomenon following genotoxin exposure. It also bears consideration that the ATM and ATR-related kinase DNA-PK has recently been shown to phosphorylate Chk2 as well (Li and Stern, 2005).

In response to replication block and UV light, ATR activates Chk1 (Liu et al., 2000). While Chk1 phosphorylation in response to IR appears somewhat reduced compared to UV-induced response (Zhou and Elledge, 2000), Chk1 is required for activation of G2 arrest in response to IR (Liu et al., 2000). MMR-deficient cells fail to activate Chk1 in

response to MNNG doses resulting in MMR-dependent G2 arrest (Adamson et al., 2005; Stojic et al., 2004b). Here, we show that high-dose MNNG exposure results in the phosphorylation of Chk1 via a MMR-independent mechanism and Chk1 is required to establish G2 arrest in response to high-dose MNNG exposure. Taken together, these findings indicate that while Chk1 is activated through differing mechanisms depending upon the extent of MNNG-induced lesions, Chk1 is an indispensable component in the G2 checkpoint machinery.

In contrast to our previous study where we observed that RNAi-induced depletion of Chk2 resulted in diminished G2 checkpoint activation following moderate doses of MNNG (Adamson et al., 2005), we document that Chk2-deficient cells show no observable perturbation in G2 arrest after high doses of MNNG but Chk1 is required for establishment of this checkpoint. Despite their structural dissimilarity, common downstream targets for Chk1 and Chk2, such as p53, Cdc25A and Cdc25C exist (Chehab et al., 2000; Falck et al., 2001; Matsuoka et al., 1998; Sanchez et al., 1997; Shieh et al., 2000; Zhao et al., 2002). By using peptide libraries to assess Chk1 and Chk2 substrate specificity, O'Neill et al. (2002) found substantial differences between these two Ser/Thr kinases. This finding supports the view that Chk1 and Chk2 are only partially redundant in function and that there are likely distinct damage-responsive Chk1 or Chk2-dependent pathways. We documented that 25 μM MNNG results in a quantitatively higher level of phosphorylated Chk1 when compared to response to 5 μM MNNG in two distinct cell lines (*e.g.*, EBS-7, HCT116+ch3). It is therefore possible that, in response to high-dose MNNG exposure, Chk1-dependent checkpoint pathway(s) are activated that are either inactive or minimally active during response to lower doses of MNNG. In this scenario, Chk2 activity would be required to fully activate the G2 checkpoint in response to moderate doses of MNNG by promoting full activation of redundant pathways or activating other Chk2-dependent mechanisms. Conversely, heightened Chk1 activity produced during response to high-dose may override the Chk2 requirement observed at lower doses of MNNG. This effect is possible by either potently activating redundant pathways or triggering other non-redundant mechanisms not activated in response to moderate-dose exposure. Clearly, a more comprehensive understanding of pathways that establish the G2 checkpoint is needed to more precisely interpret the functional

contribution of Chk1 and Chk2 to the triggering of this checkpoint.

Molecular basis of response to MNNG

MNNG exposure results in the methylation of multiple nucleophilic centers within the DNA molecule. N-methylated purines (N^3A, N^7G) are recognized by specific DNA glycosylases and are repaired by base-excision repair (BER), while O^6MeG is repaired by both direct repair and excision repair mechanisms. The DNA repair protein MGMT is responsible for direct repair of O^6MeG by directly demethylation. Additionally, the MMR system recognizes O^6MeG in either O6Me:T or O6Me:C base pairs (Duckett et al., 1996; Griffin et al., 1994). Persistent O^6MeG lesions are widely viewed as the lesion that triggers MMR-dependent checkpoint signaling (Bellacosa, 2001; Stojic et al., 2004a).

In response to high-dose MNNG exposure, however, there is no apparent requirement for MMR to trigger effective checkpoint signaling. This suggests that lesions other than O^6MeG activate checkpoint mechanisms. Methyl-methane sulfonate (MMS) is an S_N2 alkylating agent that primarily alkylates the N^3 position of adenine and N^7 position of guanine but alkylates the O^6 positions of guanine to a very small extent. Resultant MMS-generated N^3A and N^7G adducts are primarily repaired by BER. During BER, glycosylases hydrolyze the glycosidic bond between the nitrogenous base and the deoxyribose moiety in the DNA backbone thus creating an apurinic/apyrimidinic (AP) site. Further, since base alkylation weakens the glycosidic bond (Loeb and Preston, 1986), AP sites can arise without glycosylase activity. AP sites are subsequently recognized by an endonuclease that catalyzes AP site-directed strand scission (Demple et al., 1991). *In vitro* studies indicate that ligation of the newly synthesized DNA strand is the rate-limiting step in BER (Srivastava et al., 1998; Sung and Mosbaugh, 2003) explaining the occurrence of strand breaks in cells exposed to both S_N1 and S_N2 alkylators (Schwartz, 1989).

We have previously shown that 25 μM MNNG induces rapid catalytic activation of ATM and accumulation of DNA strand breaks as scored by Comet assay (Adamson et al., 2002). Stojic et al (Stojic et al., 2005) recently showed that formation of γH2AX foci and activation of Chk1/2 also occur rapidly after high-dose MNNG exposure. Whereas both

Molecular Pharmacology Fast Forward. Published on June 30, 2005 as DOI: 10.1124/mol.105.013888
This article has not been copyedited and formatted. The final version may differ from this version.

ATM activation and γH2AX are correlated with the presence of double strand breaks (DSBs) in the genome (Abraham, 2001; Pilch et al., 2003), these biochemical events indicate that DSBs occur in response to high-dose MNNG exposure. DSBs generated by alkylators are due to the simultaneous processing of clustered AP sites on opposite DNA strands (Lomax et al., 2004) and their abundance would be expected to be proportional to initial lesion load. However, given the ATM-independent nature of high-dose MNNG G2 checkpoint activation, it is unlikely that MNNG-induced DSBs are the dominant lesion that triggers activation of this checkpoint.

Due to persistent N-alkylated bases and AP sites, MMS exposure results in the stalling of DNA replication (Tercero and Diffley, 2001). Electron microscopy has revealed that replication fork stalling results in the generation of long regions of single-stranded DNA (ssDNA) attributed to asymmetric DNA synthesis occurs during replication of damaged template (Sogo et al., 2002). The ATR/ATRIP complex binds to the ssDNA binding protein RPA and that this association promotes localization of ATR to sites of stalled replication (Zou and Elledge, 2003). While the importance of the recruitment of ATR to ssDNA remains in question (Ball et al., 2005), it is clear that ATR responds to stalled replication by activating Chk1 and a consequential checkpoint response (Sanchez et al., 1997; Liu et al, 2000; Zhao and Piwnica-Worms, 2001). Thus, it is formally possible that stalled replication is the dominant lesion to which the cells trigger a checkpoint response following high-dose MNNG exposure.

Acknowledgements

The authors thank Drs. A.W. Adamson and R. Baskaran for helpful insights and comments during performance of this study. We also thank Dr. Ray Braquet and Ms. Megan Bronson for technical assistance.

Molecular Pharmacology Fast Forward. Published on June 30, 2005 as DOI: 10.1124/mol.105.013888
This article has not been copyedited and formatted. The final version may differ from this version.

References

Abraham RT (2001) Cell cycle checkpoint signaling through the ATM and ATR kinases. *Genes Dev* **15**:2177-96.

Adamson AW, Beardsley DI, Kim WJ, Gao Y, Baskaran R and Brown KD (2005) Methylator-induced, Mismatch Repair-dependent G2 Arrest Is Activated through Chk1 and Chk2. *Mol Biol Cell* **16**:1513-26.

Adamson AW, Kim WJ, Shangary S, Baskaran R and Brown KD (2002) ATM is activated in response to MNNG-induced DNA alkylation. *J Biol Chem* **277**:38222-28229.

Ahn JY, Schwarz JK, Piwnica-Worms H and Canman CE (2000) Threonine 68 phosphorylation by ataxia telangiectasia mutated is required for efficient activation of Chk2 in response to ionizing radiation. *Cancer Res* **60**:5934-6.

Allen DM, van Praag H, Ray J, Weaver Z, Winrow CJ, Carter TA, Braquet R, Harrington E, Ried T, Brown KD, Gage FH and Barlow C (2001) Ataxia telangiectasia mutated is essential during adult neurogenesis. *Genes Dev* **15**:554-66.

Ball HL, Myers JS and Cortez D (2005) ATRIP Binding to RPA-ssDNA Promotes ATR-ATRIP Localization but Is Dispensable for Chk1 Phosphorylation. *Mol Biol Cell*. (in press)

Bellacosa A (2001) Functional interactions and signaling properties of mammalian DNA mismatch repair proteins. *Cell Death Differ* **8**:1076-92.

Branch P, Aquilina G, Bignami M and Karran P (1993) Defective mismatch binding and a mutator phenotype in cells tolerant to DNA damage. *Nature* **362**:652-4.

Castedo M, Perfettini JL, Roumier T, Yakushijin K, Horne D, Medema R and Kroemer G (2004) The cell cycle checkpoint kinase Chk2 is a negative regulator of mitotic catastrophe. *Oncogene* **23**:4353-61.

Chehab NH, Malikzay A, Appel M and Halazonetis TD (2000) Chk2/hCds1 functions as a DNA damage checkpoint in G(1) by stabilizing p53. *Genes Dev* **14**:278-88.

Cortez D, Guntuku S, Qin J and Elledge SJ (2001) ATR and ATRIP: partners in checkpoint signaling. *Science* **294**:1713-6.

Demple B, Herman T and Chen DS (1991) Cloning and expression of APE, the cDNA encoding the major human apurinic endonuclease: definition of a family of DNA repair enzymes. *Proc Natl Acad Sci U S A* **88**:11450-4.

Duckett DR, Drummond JT, Murchie AI, Reardon JT, Sancar A, Lilley DM and Modrich P (1996) Human MutSalpha recognizes damaged DNA base pairs containing O6-methylguanine, O4-methylthymine, or the cisplatin-d(GpG) adduct. *Proc Natl Acad Sci U S A* **93**:6443-7.

Falck J, Mailand N, Syljuasen RG, Bartek J and Lukas J (2001) The ATM-Chk2-Cdc25A checkpoint pathway guards against radioresistant DNA synthesis. *Nature* **410**:842-7.

Goldmacher VS, Cuzick RA, Jr. and Thilly WG (1986) Isolation and partial

characterization of human cell mutants differing in sensitivity to killing and mutation by methylnitrosourea and N- methyl-N'-nitro-N-nitrosoguanidine. *J Biol Chem* **261**:12462-71.

Graves PR, Yu L, Schwarz JK, Gales J, Sausville EA, O'Connor PM and Piwnica-Worms H (2000) The Chk1 protein kinase and the Cdc25C regulatory pathways are targets of the anticancer agent UCN-01. *J Biol Chem* **275**:5600-5.

Griffin S, Branch P, Xu YZ and Karran P (1994) DNA mismatch binding and incision at modified guanine bases by extracts of mammalian cells: implications for tolerance to DNA methylation damage. *Biochemistry* **33**:4787-93.

Hawn MT, Umar A, Carethers JM, Marra G, Kunkel TA, Boland CR and Koi M (1995) Evidence for a connection between the mismatch repair system and the G2 cell cycle checkpoint. *Cancer Res* **55**:3721-5.

Jaiswal AS, Multani AS, Pathak S and Narayan S (2004) N-methyl-N'-nitro-N-nitrosoguanidine-induced senescence-like growth arrest in colon cancer cells is associated with loss of adenomatous polyposis coli protein, microtubule organization, and telomeric DNA. *Mol Cancer* **3**:3.

Jallepalli PV, Lengauer C, Vogelstein B and Bunz F (2003) The Chk2 tumor suppressor is not required for p53 responses in human cancer cells. *J Biol Chem* **278**:20475-9.

Kalamegham R, Warmels-Rodenhiser S, MacDonald H and Ebisuzaki K (1988) O6-methylguanine-DNA methyltransferase-defective human cell mutant: O6-methylguanine, DNA strand breaks and cytotoxicity. *Carcinogenesis* **9**:1749-53.

Karran P and Bignami M (1992) Self-destruction and tolerance in resistance of mammalian cells to alkylation damage. *Nucleic Acids Res* **20**:2933-40.

Kat A, Thilly WG, Fang WH, Longley MJ, Li GM and Modrich P (1993) An alkylation-tolerant, mutator human cell line is deficient in strand- specific mismatch repair. *Proc Natl Acad Sci U S A* **90**:6424-8.

Kharbanda S, Saleem A, Datta R, Yuan ZM, Weichselbaum R and Kufe D (1994) Ionizing radiation induces rapid tyrosine phosphorylation of p34cdc2. *Cancer Res* **54**:1412-1414.

Koi M, Umar A, Chauhan DP, Cherian SP, Carethers JM, Kunkel TA and Boland CR (1994) Human chromosome 3 corrects mismatch repair deficiency and microsatellite instability and reduces N-methyl-N'-nitro-N- nitrosoguanidine tolerance in colon tumor cells with homozygous hMLH1 mutation. *Cancer Res* **54**:4308-12.

Lee MS, Ogg S, Xu M, Parker LL, Donoghue DJ, Maller JL and Piwnica-Worms H (1992) cdc25+ encodes a protein phosphatase that dephosphorylates p34cdc2. *Mol. Biol. Cell* **3**:73-84.

Li J and Stern DF (2005) Regulation of CHK2 by DNA-dependent protein kinase. *J Biol Chem* **280**:12041-50.

Liu Q, Guntuku S, Cui XS, Matsuoka S, Cortez D, Tamai K, Luo G, Carattini-Rivera S,

DeMayo F, Bradley A, Donehower LA and Elledge SJ (2000) Chk1 is an essential kinase that is regulated by Atr and required for the G(2)/M DNA damage checkpoint. *Genes Dev* **14**:1448-59.

Loeb LA and Preston BD (1986) Mutagenesis by apurinic/apyrimidinic sites. *Annu Rev Genet* **20**:201-30.

Lomax ME, Cunniffe S and O'Neill P (2004) Efficiency of repair of an abasic site within DNA clustered damage sites by mammalian cell nuclear extracts. *Biochemistry* **43**:11017-26.

Lopez-Girona A, Furnari B, Mondesert O and Russell P (1999) Nuclear localization of Cdc25 is regulated by DNA damage and a 14-3-3 protein. *Nature* **397**:172-175.

Masrouha N, Yang L, Hijal S, Larochelle S and Suter B (2003) The Drosophila chk2 gene loki is essential for embryonic DNA double-strand-break checkpoints induced in S phase or G2. *Genetics* **163**:973-82.

Matsuoka S, Huang M and Elledge SJ (1998) Linkage of ATM to cell cycle regulation by the Chk2 protein kinase. *Science* **282**:1893-7.

Matsuoka S, Rotman G, Ogawa A, Shiloh Y, Tamai K and Elledge SJ (2000) Ataxia telangiectasia-mutated phosphorylates Chk2 in vivo and in vitro. *Proc Natl Acad Sci U S A* **97**:10389-10394.

Meikrantz W, Bergom MA, Memisoglu A and Samson L (1998) O6-alkylguanine DNA lesions trigger apoptosis. *Carcinogenesis* **19**:369-72.

Modrich P and Lahue R (1996) Mismatch repair in replication fidelity, genetic recombination, and cancer biology. *Annu Rev Biochem* **65**:101-33.

O'Neill T, Giarratani L, Chen P, Iyer L, Lee CH, Bobiak M, Kanai F, Zhou BB, Chung JH and Rathbun GA (2002) Determination of substrate motifs for human Chk1 and hCds1/Chk2 by the oriented peptide library approach. *J Biol Chem* **277**:16102-15.

Paules RS, Levedakou EN, Wilson SJ, Innes CL, Rhodes N, Tlsty TD, Galloway DA, Donehower LA, Tainsky MA and Kauffmann WK (1995) Defective G2 checkpoint function in cells from individuals with familial cancer syndromes. *Cancer Res.* **55**:1763-1773.

Peng CY, Graves PR, Thoma RS, Wu Z, Shaw AS and Piwnica-Worms H (1997) Mitotic and G2 checkpoint control: regulation of 14-3-3 protein binding by phosphorylation of Cdc25C on serine-216. *Science* **277**:1501-5.

Pilch DR, Sedelnikova OA, Redon C, Celeste A, Nussenzweig A and Bonner WM (2003) Characteristics of gamma-H2AX foci at DNA double-strand breaks sites. *Biochem Cell Biol* **81**:123-9.

Sanchez Y, Wong C, Thoma RS, Richman R, Wu Z, Piwnica-Worms H and Elledge SJ (1997) Conservation of the Chk1 checkpoint pathway in mammals: linkage of DNA damage to Cdk regulation through Cdc25. *Science* **277**:1497-501.

Sarkaria JN, Busby EC, Tibbetts RS, Roos P, Taya Y, Karnitz LM and Abraham RT

(1999) Inhibition of ATM and ATR kinase activities by the radiosensitizing agent, caffeine. *Cancer Res* **59**:4375-82.

Sarkaria JN, Tibbetts RS, Busby EC, Kennedy AP, Hill DE and Abraham RT (1998) Inhibition of phosphoinositide 3-kinase related kinases by the radiosensitizing agent wortmannin. *Cancer Res.* **58**:4375-4382.

Schwartz JL (1989) Monofunctional alkylating agent-induced S-phase-dependent DNA damage. *Mutat Res* **216**:111-8.

Shieh SY, Ahn J, Tamai K, Taya Y and Prives C (2000) The human homologs of checkpoint kinases Chk1 and Cds1 (Chk2) phosphorylate p53 at multiple DNA damage-inducible sites. *Genes Dev* **14**:289-300.

Singh SV, Herman-Antosiewicz A, Singh AV, Lew KL, Srivastava SK, Kamath R, Brown KD, Zhang L and Baskaran R (2004) Sulforaphane-induced G2/M phase cell cycle arrest involves checkpoint kinase 2-mediated phosphorylation of cell division cycle 25C. *J Biol Chem* **279**:25813-22.

Sogo JM, Lopes M and Foiani M (2002) Fork reversal and ssDNA accumulation at stalled replication forks owing to checkpoint defects. *Science* **297**:599-602.

Srivastava DK, Berg BJ, Prasad R, Molina JT, Beard WA, Tomkinson AE and Wilson SH (1998) Mammalian abasic site base excision repair. Identification of the reaction sequence and rate-determining steps. *J Biol Chem* **273**:21203-9.

Stojic L, Brun R and Jiricny J (2004a) Mismatch repair and DNA damage signalling. *DNA Repair (Amst)* **3**:1091-101.

Stojic L, Cejka P and Jiricny J (2005) High Doses of S(N)1 Type Methylating Agents Activate DNA Damage Signaling Cascades that are Largely Independent of Mismatch Repair. *Cell Cycle* **4**.

Stojic L, Mojas N, Cejka P, Di Pietro M, Ferrari S, Marra G and Jiricny J (2004b) Mismatch repair-dependent G2 checkpoint induced by low doses of SN1 type methylating agents requires the ATR kinase. *Genes Dev* **18**:1331-44.

Strausfeld U, Labbe JC, Fesquet D, Cavadore JC, Picard A, Sadhu K, Russell P and Doree M (1991) Dephosphorylation and activation of a p34cdc2/cyclin B complex in vitro by human CDC25 protein. *Nature* **351**:242-5.

Sung JS and Mosbaugh DW (2003) Escherichia coli uracil- and ethenocytosine-initiated base excision DNA repair: rate-limiting step and patch size distribution. *Biochemistry* **42**:4613-25.

Tercero JA and Diffley JF (2001) Regulation of DNA replication fork progression through damaged DNA by the Mec1/Rad53 checkpoint. *Nature* **412**:553-7.

Umar A, Koi M, Risinger JI, Glaab WE, Tindall KR, Kolodner RD, Boland CR, Barrett JC and Kunkel TA (1997) Correction of hypermutability, N-methyl-N'-nitro-N-nitrosoguanidine resistance, and defective DNA mismatch repair by introducing chromosome 2 into human tumor cells with mutations in MSH2 and MSH6. *Cancer Res* **57**:3949-55.

Wang Y and Qin J (2003) MSH2 and ATR form a signaling module and regulate two branches of the damage response to DNA methylation. *Proc Natl Acad Sci U S A.*

Wei JH, Chou YF, Ou YH, Yeh YH, Tyan SW, Sun TP, Shen CY and Shieh SY (2005) TTK/hMps1 participates in the regulation of DNA damage checkpoint response by phosphorylating CHK2 on threonine 68. *J Biol Chem* **280**:7748-57.

Xu B, Kim ST, Lim DS and Kastan MB (2002) Two molecularly distinct g(2)/m checkpoints are induced by ionizing irradiation. *Mol Cell Biol* **22**:1049-59.

Yu Q, La Rose J, Zhang H, Takemura H, Kohn KW and Pommier Y (2002) UCN-01 inhibits p53 up-regulation and abrogates gamma-radiation-induced G(2)-M checkpoint independently of p53 by targeting both of the checkpoint kinases, Chk2 and Chk1. *Cancer Res* **62**:5743-8.

Zhao H and Piwnica-Worms H (2001) ATR-mediated checkpoint pathways regulate phosphorylation and activation of human Chk1. *Mol Cell Biol* **21**:4129-39.

Zhao H, Watkins JL and H. P-W (2002) Disruption of the checkpoint kinase 1/cell division cycle 25A pathway abrogates ionizing radiation-induced S and G2 checkpoints. *Proc Natl Acad Sci U S A.* **99**:14795-14800.

Zhou BB and Elledge SJ (2000) The DNA damage response: putting checkpoints in perspective. *Nature* **408**:433-9.

Ziv Y, Bar-Shira A, Pecker I, Russell P, Jorgensen TJ, Tsarfati I and Shiloh Y (1997) Recombinant ATM protein complements the cellular A-T phenotype. *Oncogene* **15**:159-67.

Zou L and Elledge SJ (2003) Sensing DNA damage through ATRIP recognition of RPA-ssDNA complexes. *Science* **300**:1542-8.

Molecular Pharmacology Fast Forward. Published on June 30, 2005 as DOI: 10.1124/mol.105.013888
This article has not been copyedited and formatted. The final version may differ from this version.

Footnotes

This study was funded by a grant from the NIH (R01-CA102289) to KDB.

Molecular Pharmacology Fast Forward. Published on June 30, 2005 as DOI: 10.1124/mol.105.013888
This article has not been copyedited and formatted. The final version may differ from this version.

Figure Legends

Figure 1. ***High-dose MNNG exposure activates an ATM- and MMR-independent G2 arrest that is abrogated by the pharmacological inhibitors caffeine and UCN-01.*** **A**. ATM-deficient EBS-7 fibroblasts were either mock-treated or exposed to 5 or 25μM MNNG, harvested at 48 hr, fixed, stained with propidium iodide, and analyzed by flow cytometry. The percentage of cells in the histogram containing 4N DNA content is indicated. **B.** ATM-proficient YZ-5 fibroblasts were treated and analyzed as outlined in A. **C.** MMR-deficient HCT116 colorectal tumor cells were treated and analyzed as outlined in A. **D**. MMR-proficient HCT116+ch3 cells were treated and analyzed as outlined in A. **E**. EBS-7 cells were pretreated with 5mM caffeine for 1 hr prior to 25μM MNNG exposure and caffeine was maintained in the growth medium throughout the incubation period. Alternatively, EBS-7 cells were pretreated with 500nM UCN-01 for 45 min prior to MNNG exposure and UCN-01 was maintained in the growth medium throughout the incubation period. Mock treated, 25 μM MNNG only treated, 25 μM MNNG+caffeine, caffeine only, 25 μM MNNG+UCN-01, and UCN-01 only treated cells were harvested 48 hr after MNNG treatment, fixed, stained with propidium iodide and analyzed by flow cytometry. The percentage of cells displaying a 4N DNA content is noted. **F**. HCT116 cells were treated and analyzed as outlined in E.

Figure 2. ***Nuclear exclusion of Cdc25C and accumulation of inactive Cdc2 occur in an ATM- and MMR-independent manner following high-dose MNNG exposure.*** **A**. EBS-7 cells were either mock treated (lane 1), 5μM MNNG-treated (lane 2), 25μM MNNG-treated (lane 3), pretreated for 1 hr and maintained on 5mM caffeine following 25μM MNNG treatment (lane 4), caffeine-treated only (lane 5), pretreated for 45 min and maintained on UCN-01 following 25μM MNNG treatment (lane 6), and UCN-01-treated only (lane 7). Cells were harvested 48 hr following MNNG exposure and subsequently fractionated into nuclear and cytoplasmic fractions. These nuclear fractions were immunoblotted with anti-Cdc25C (top) or SMC1 (bottom; nuclear fraction loading control). **B.** HCT116 cells were analyzed as outlined in A. **C**. EBS-7 cells were treated as outlined in A; however, total cell lysates were formed from the harvested cells and

these were subjected to immunoblot analysis with phospho-Tyr15 Cdc2 specific antibody (top) or anti-total Cdc2 (bottom) to confirm equal protein abundance. **D**. HCT116 cells were analyzed as outlined in C.

Figure 3. ***Neither ATM nor MMR are required for activation/phosphorylation of Chk1 or Chk2 following high-dose exposure of MNNG.*** **A**. EBS-7 cells were either mock treated (lane 1), treated with 5μM MNNG (lane 2), or treated with 25μM MNNG (lane 3). Cells were harvested 48 hr after MNNG exposure and the extracts were immunoblotted with phospho-Ser317 Chk1 specific antibody (top) or anti-total Chk1 (bottom). **B.** HCT116 were treated and analyzed as in A. **C**. EBS-7 extracts were analyzed by immunoblotting with phospho-Thr68 Chk2 specific antibody (top) or anti-total Chk2 (bottom). **D.** HCT116 extracts were analyzed as outlined in C.

Figure 4. ***ATR is required for Chk1 activation of and establishment of G2 arrest following high-dose MNNG treatment.*** **A.** HCT116 (lanes 1,2) or $ATR^{flox/-}$ (lanes 3,4) were either mock-infected (lanes 1,3) or infected with adenovirus (lanes 2,4) expressing Cre-recombinase (Ad-Cre). 48 hr after viral infection cells were harvested, lysates formed and subjected to immunoblot analysis with anti-ATR (top), anti-ATM (middle), or anti-tubulin (bottom) as a protein loading control. **B**. $ATR^{flox/-}$ cells were either mock treated (lane 1), 25μM MNNG-treated (lane 2), 25μM MNNG treated 48 hr after Ad-Cre infection (lane 3), or infected with Ad-Cre only (lane 4). 48 hr after MNNG exposure cells were harvested, extracts formed, and subsequently immunoblotted with phospho-Ser317 Chk1 specific antibody (top) or anti-total Chk1 (bottom). **C**. Extracts outlined in B were immunoblotted with phospho-Thr68 Chk2 specific antibody (top) or anti-total Chk2 (bottom). **D**. $ATR^{flox/-}$ cells were either mock-treated, 25μM MNNG-treated, 25μM MNNG treated 48 hr after Ad-Cre infection, or were only Ad-Cre infected. Cells were harvested 48 hr after MNNG exposure, fixed, stained with propidium iodide, and subsequently analyzed by flow cytometry. The percentage of cells containing 4N DNA is indicated. **E**. HCT116 cells were treated and analyzed as outlined in D. **F.** Plotted are the mean percentages of G2 arrested cells measured in three independent experiments

Molecular Pharmacology Fast Forward. Published on June 30, 2005 as DOI: 10.1124/mol.105.013888
This article has not been copyedited and formatted. The final version may differ from this version.

conducted on 25 μM MNNG treated HCT116, uninfected $ATR^{flox/-}$, and Ad-Cre infected $ATR^{flox/-}$ cells. Error bars = 1.0 SD.

Figure 5. ***Chk2 is not required for activation of G2 arrest in response to high-dose MNNG exposure.*** **A.** Extracts of HCT116 (lane 1) and HCT116 $Chk2^{-/-}$ (lane 2) cells were immunoblotted with anti-Chk2 (top) or anti-Chk1 (bottom) antibody. **B**. HCT116 $Chk2^{-/-}$ cells were either mock treated, 25μM MNNG-treated, pretreated for 45 min and maintained on 500 nM UCN-01 during and after 25μM MNNG treatment, or treated with 500 nM UCN-01 only. 48 hr after MNNG exposure cells were harvested, fixed, stained with propidium iodide, and analyzed by flow cytometry. The percentage of cells with 4N DNA content is indicated.

Figure 6. ***RNAi-induced depletion of Chk1 results in diminished establishment of G2 arrest following high-dose MNNG exposure.*** **A**. HCT116 $Chk2^{-/-}$ cells were either mock-transfected (lane1), transfected with non-target control siRNA (lane 2), or transfected with pooled Chk1-specific siRNA (lane 3). 48 hr post-transfection, cells were immunoblotted with anti-total Chk1 (top) or anti-tubulin (bottom) to confirm equivalent loading. The fold reduction in Chk1 expression is indicated as measured by analysis of exposed autoradiography films. **B**. HCT116 $Chk2^{-/-}$ cells were either mock-transfected, transfected with non-target siRNA or transfected with Chk1-specific siRNA. Following this, cultures were evenly divided and cells were mock-treated or exposed to 25μM MNNG, harvested 48 hr later and analyzed by flow cytometry. The percentage of cells containing 4N DNA content is indicated. **C**. HCT116+ch3 cells were either mock treated (lane 1), 5μM MNNG-treated (lane 2), or 25μM MNNG-treated (lane 3). Cells were harvested 48 hr after drug treatment, lysed, and immunoblotted with phospho-Ser317 Chk1 specific antibody (top) and anti-total Chk1 (bottom). The relative intensity of the phosphorylated Chk1 signal is indicated. **D**. HCT116+ch3 cells were either mock transfected (lane1), transfected with non-target control siRNA (lane 2), or transfected with pooled Chk1-specific siRNA (lane 3) and 48 hr after transfection the cell extracts were immunoblotted with anti-total Chk1 (top) and anti-tubulin (bottom). **E**. HCT116+ch3 cells were either mock-transfected, transfected with non-target control

siRNA, or transfected with Chk1-specific siRNA. Following this, cultures were divided into three equal pools. These pools were either mock-treated, treated with 5 μM MNNG or 25μM MNNG, harvested 48 hr later and analyzed by flow cytometry. The percentage of cells display a 4N DNA content is indicated. **F.** Plotted are the mean percentages of G2 arrested cells measured in three independent experiments conducted on 25 μM MNNG treated HCT116+ch3 transfected with either control siRNA or Chk1 siRNA, or HCT116+ch3 cells transfected with Chk1 siRNA and treated with 5 μM MNNG. Error bars = 1.0 SD.

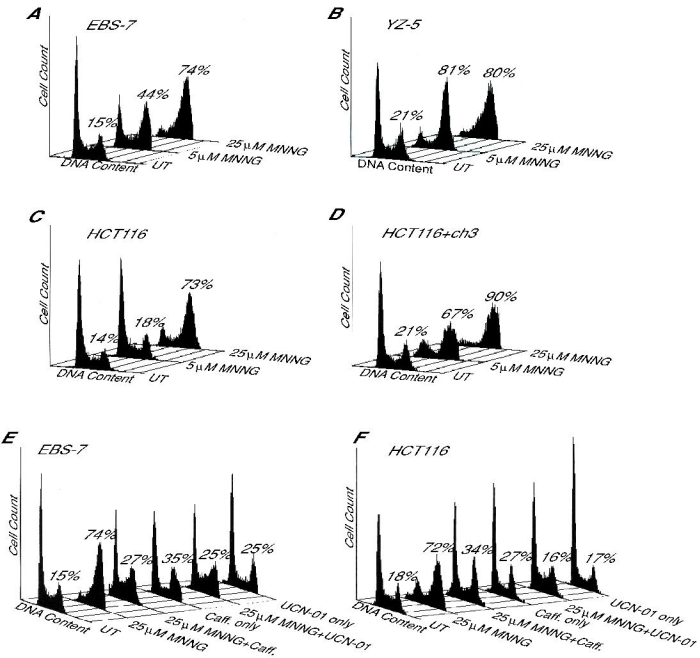
A
EBS-7
Cell Count
74%
44%
15%
25 μM MNNG
5 μM MNNG
DNA Content
UT
B
YZ-5
Cell Count
81%
80%
21%
25 μM MNNG
5 μM MNNG
DNA Content
UT
C
HCT116
Cell Count
73%
18%
14%
25 μM MNNG
5 μM MNNG
DNA Content
UT
D
HCT116+ch3
Cell Count
90%
67%
21%
25 μM MNNG
5 μM MNNG
DNA Content
UT
E
EBS-7
Cell Count
74%
27%
35%
25%
25%
15%
UCN-01 only
25 μM MNNG+UCN-01
Caff. only
25 μM MNNG+Caff.
DNA Content
UT
25 μM MNNG
F
HCT116
Cell Count
72%
34%
27%
16%
17%
18%
UCN-01 only
25 μM MNNG+UCN-01
Caff. only
25 μM MNNG+Caff.
DNA Content
UT
25 μM MNNG

Fig. 1

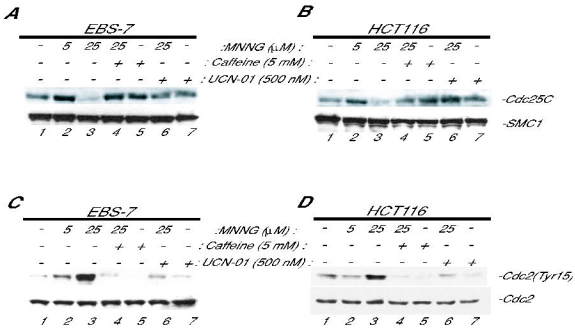
A
EBS-7
- 5 25 25 - 25 - :MNNG (μM) :
- - - + + - - : Caffeine (5 mM) :
- - - - - + + : UCN-01 (500 nM) :
1 2 3 4 5 6 7
B
HCT116
- 5 25 25 - 25 -
- - - + + - -
- - - - - + +
-Cdc25C
-SMC1
1 2 3 4 5 6 7
C
EBS-7
- 5 25 25 - 25 - :MNNG (μM) :
- - - + + - - : Caffeine (5 mM) :
- - - - - + + : UCN-01 (500 nM) :
1 2 3 4 5 6 7
D
HCT116
- 5 25 25 - 25 -
- - - + + - -
- - - - - + +
-Cdc2(Tyr15)
-Cdc2
1 2 3 4 5 6 7

Fig. 2

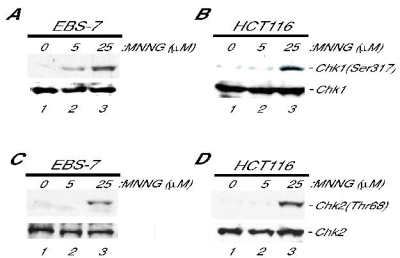
A
EBS-7
0 5 25 :MNNG (μM)
1 2 3
B
HCT116
0 5 25 :MNNG (μM)
- Chk1(Ser317)
- Chk1
1 2 3
C
EBS-7
0 5 25 :MNNG (μM)
1 2 3
D
HCT116
0 5 25 :MNNG (μM)
- Chk2(Thr68)
- Chk2
1 2 3

Fig. 3

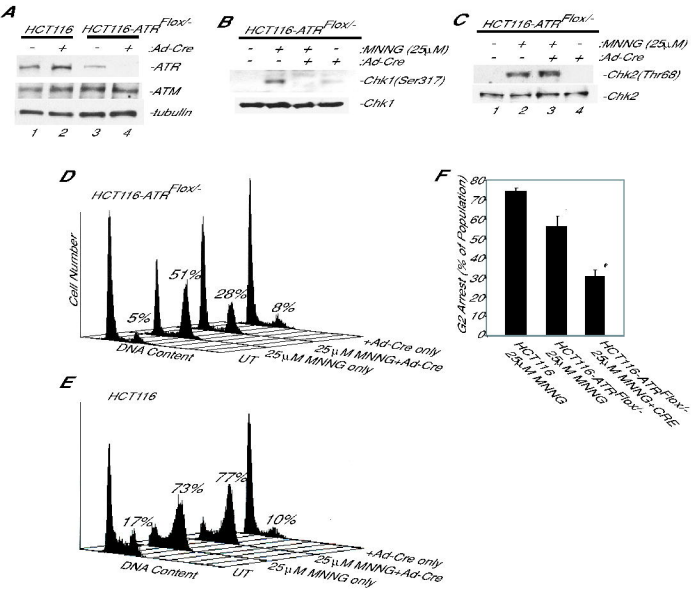
A
HCT116
HCT116-ATRFlox/-
-Ad-Cre
-ATR
-ATM
-tubulin
1 2 3 4
B
HCT116-ATRFlox/-
-MNNG (25μM)
-Ad-Cre
-Chk1(Ser317)
-Chk1
C
HCT116-ATRFlox/-
-MNNG (25μM)
-Ad-Cre
-Chk2(Thr68)
-Chk2
1 2 3 4
D
HCT116-ATRFlox/-
Cell Number
5%
51%
28%
8%
DNA Content
UT
+Ad-Cre only
25μM MNNG only
25μM MNNG+Ad-Cre
E
HCT116
17%
73%
77%
10%
DNA Content
UT
+Ad-Cre only
25μM MNNG only
25μM MNNG+Ad-Cre
F
G2 Arrest (% of Population)
0
10
20
30
40
50
60
70
80
HCT116 25μM MNNG
HCT116-ATR 25μM MNNG
HCT116-ATRFlox/-
HCT116-ATRFlox/- 25μM MNNG+CRE

Fig. 4

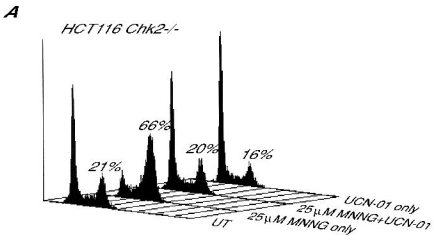
A
HCT116 Chk2-/-
21%
66%
20%
16%
UT
25μM MNNG only
25μM MNNG+UCN-01
UCN-01 only

Fig. 5

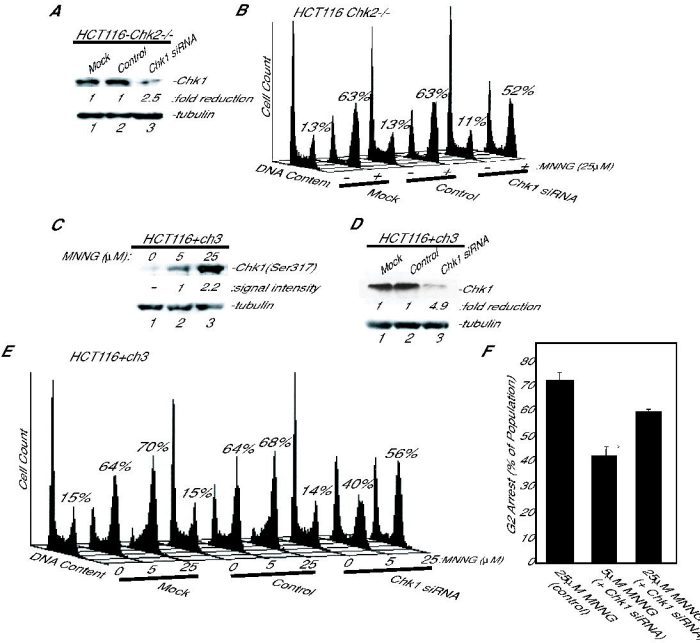
A
HCT116-Chk2-/-
Mock
Control
Chk1 siRNA
-Chk1
1 1 2.5 :fold reduction
-tubulin
1 2 3
B
HCT116 Chk2-/-
Cell Count
13%
63%
13%
63%
11%
52%
MNNG (25μM)
DNA Content
Mock
Control
Chk1 siRNA
C
HCT116+ch3
MNNG (μM): 0 5 25
-Chk1(Ser317)
- 1 2.2 :signal intensity
-tubulin
1 2 3
D
HCT116+ch3
Mock
Control
Chk1 siRNA
-Chk1
1 1 4.9 :fold reduction
-tubulin
1 2 3
E
HCT116+ch3
Cell Count
15%
64%
70%
15%
64%
68%
14%
40%
56%
DNA Content
0 5 25 0 5 25 0 5 25 MNNG (μM)
Mock
Control
Chk1 siRNA
F
G2 Arrest (% of Population)
0 10 20 30 40 50 60 70 80
25μM MNNG (control)
5μM MNNG (+ Chk1 siRNA)
25μM MNNG (+ Chk1 siRNA)

Fig. 6